Static and Dynamic Paraelectric Behavior of ⟨110⟩ Off-Center Ag^+ Ions in RbCl and RbBr†

Siegmar Kapphan* and Fritz Lüty
Physics Department, University of Utah, Salt Lake City, Utah 84112
(Received 10 April 1972)

Controversial results and considerable uncertainty have existed so far on the question of possible off-center behavior and paraelectric properties of Ag^+ ions in RbCl and RbBr. In a comprehensive study, the static and dynamic paraelectric properties of both systems at low temperature are investigated, using the electrodichroism of the Ag^+ uv absorption. The static electro-optical measurements, performed for three field orientations at the A, D_1, and D_2 band, reveal for both systems paraelectric behavior from ⟨110⟩-oriented dipoles with dipole moment values of 0.78 and 0.95 e Å for RbCl : Ag^+ and RbBr : Ag^+, respectively. Measurements on the time-dependent electrodichroism after rapid changes of the electric field show the existence of two relaxation processes with rates different by several orders of magnitude. The observed relative amount of both processes depends strongly on the applied-field direction. This complex relaxation behavior can be quantitatively accounted for by a ⟨110⟩ dipole model which is based on predominance of 90° reorientation over 60° reorientation. This behavior, which cannot be understood for a dipole in an octahedral crystal field, is attributed to the dressing of the dipole by a strong E_g lattice distortion, which allows easy 90° rotation within a {100} plane, but inhibits the change of this plane by 60° dipole reorientation. The observed temperature and field dependence of the relaxation rates indicate reorientation by tunneling processes at $T < 5$ °K, and classical thermally activated reorientation at higher temperature. Several of the earlier discrepancies can be explained by this ⟨110⟩ dipole and two-relaxation-time model.

I. INTRODUCTION

Two types of paraelectric impurities in alkali halides, discovered within the last decade, have attracted a great deal of experimental and theoretical interest: substitutional molecular defects, carrying an intrinsic electric-dipole moment, and substitutional point ions in noncentrosymmetric positrons, which form electric dipoles due to an off-center displacement. The cubic crystalline field produces a multiwell potential for the angular orientation of these lattice defects, the absolute minima of which determine the "equilibrium orientations" at low temperature. Tunneling among the potential wells allows reorientation and, therefore, paraelectric-dipole alignment even at very low temperatures.

The best understood "prototype" off-center defect is the Li^+ ion in KCl, which has been very thoroughly investigated both experimentally and theoretically.[1] With a large variety of experimental techniques, a high degree of consistency was achieved in determining the important paraelectric parameters of the defect: equilibrium orientation in ⟨111⟩, dipole moment $p = 1.2\ e$Å, and predominant nearest-neighbor (70°) tunneling with a matrix element of 1.1 cm^{-1} for Li^6 and 0.8 cm^{-1} for Li^7.

Soon after the discovery of the off-center effect for the small-mass Li^+ impurity system, a different group of impurities, substitutional heavy-metal ions like Ag^+ and Cu^+, came into consideration for the same effect. The first indication for their possible off-center behavior was obtained "indirectly" from systematical optical studies by the group in Frankfurt. For the Cu^+ and Ag^+ center the parity-forbidden transitions $3d^{10} \rightarrow 3d^9 4s$ and $4d^{10} \rightarrow 4d^9 5s$ were found to become partly allowed in the crystal through electron-phonon interaction with odd-parity lattice modes. This gives rise to an uv absorption with small oscillator strength ($f \sim 0.001$), which increases with the temperature.[2] In contrast to this behavior a much stronger low-temperature uv absorption was found for Cu^+ in KCl, KBr, and KI,[3] and a similarly abnormal absorption strength was found for Ag^+ in RbCl and RbBr.[4] This was interpreted to be caused by a static odd-parity distortion of the center due to an off-center position of the metal ion. After this first qualitative indication for off-center behavior, several subsequent investigations with various techniques tried to establish more quantitatively the off-center and paraelectric properties of these defects. In the following, this work is briefly reviewed for the two systems of interest here, RbCl : Ag^+ and RbBr : Ag^+.

The first experimental proof for low-temperature paraelectric behavior of the Ag^+ ion in RbCl was obtained from electrocaloric measurements by Kapphan and Lüty.[5] A dipole-moment value of $p = (0.85 \pm 0.08)\ e$Å and a relaxation time of 8×10^{-6} sec at 1.4 °K were obtained; the anisotropy of the electrocaloric effect at high fields indicated the ⟨111⟩ orientation of the dipoles. Calculations with a polarizable-point-ion model by Wilson *et al.*[6] confirmed an off-center potential for Ag^+ in RbCl, with absolute minima displaced from the center by

0.54 Å in the ⟨111⟩ directions. From paraelectric-resonance (PER) measurements by Bridges,[7] a dipole moment of $p = 0.95\ e$ Å and an upper limit for the tunneling splitting of $\Delta = 0.1\ \mathrm{cm}^{-1}$ were derived for RbCl: Ag^+. From the PER data it was concluded that the defects should have ⟨111⟩ orientation, if they reorient by nearest-neighbor tunneling, or ⟨110⟩ orientations if they reorient by next-nearest-neighbor tunneling. Nolt[8] and Kirby *et al.*[9] found in RbCl: Ag^+ three resonant-mode absorptions at 21, 26, and 37 cm^{-1} of comparable strength. They argue that the threefold structure is not compatible with a ⟨111⟩ off-center model, but could be explained by a ⟨110⟩ displaced Ag^+ center. Moreover, they show that the direction of field- and stress-induced absorption changes in the three components agrees qualitatively with the expectation for reorientation dichroism of ⟨110⟩-oriented electric and elastic dipoles. The small size of the dichroism, however, would indicate a very small (~0.1 e Å) electric-dipole moment. Dielectric measurements by Hanson *et al.*,[10] performed down to 0.3 °K, determined ⟨111⟩-oriented electric dipoles with a moment of 1 e Å. Low-temperature elastic measurements[10] indicate in contrast to this a ⟨100⟩ symmetry of the elastic dipoles.

Rollefson[11] observes a low-temperature specific-heat anomaly from Ag^+ ions in RbCl; its temperature dependence deviates strongly from a Schottky anomaly, expected for an ideal multiplet of tunneling states.[1] Integration of the anomaly yields an entropy value per Ag^+ ion of $S = k \ln 1.8$, far less than expected for a ⟨111⟩ or ⟨110⟩ dipole ($S_{111} = k \ln 8$, $S_{110} = k \ln 12$). These data indicate that only a small fraction of the total Ag^+ ions in the crystal take part in the low-temperature reorientation, and that their orientational levels are split by a tunneling splitting small compared to an effective splitting from background strain in the crystal.

The RbBr: Ag^+ system displayed no electrocaloric effect[5] and produced in the theoretical calculation a centrosymmetric potential.[6] PER and far-infrared investigations have not been done for this system. Recent electro-optical measurements by Sittig[12] performed down to 20 °K, exhibit field modulation of the electronic Ag^+ absorption proportional to $(E/T)^2$, thus giving strong indication for a dipole-reorientation dichroism. The observed anisotropy of the effect excludes ⟨100⟩ and ⟨111⟩ off-center positions, while comparison with the behavior expected for ⟨110⟩ dipoles gives a reasonable but not in any way quantitative agreement. Sittig explains this with the assumption that the Ag^+ has not really well-defined ⟨110⟩ off-center orientations, but can move along "off-center tubes" (e.g., between ⟨111⟩ and ⟨11$\bar{1}$⟩ via a ⟨110⟩ position) with a higher probability to be near a ⟨110⟩ place. From the electro-optical measurements, which were done only down to 20 °K, a dipole-moment value of $p = 0.27\ e$ Å was estimated. To connect these results with the negative electrocaloric results[5] one has to assume that the dipole reorientation (which at 20 °K has a rate $\tau^{-1} > 2 \times 10^2\ \mathrm{sec}^{-1}$) must freeze in between 20 and 4 °K. Elasto-optical measurements by Dultz and Uihlein[13] give qualitative indication for ⟨110⟩-oriented elastic dipoles.

The conclusions from the above-mentioned investigations for both systems RbCl: Ag^+ and RbBr: Ag^+ are summarized in Table I, displaying a high degree of inconsistencies and discrepancies. For RbCl: Ag^+ there exists at least general agreement from all methods used, that the ion sits, in fact, off-center and displays electric and elastic alignment at low temperatures; the electric-dipole-moment values (aside of the one derived from the ir results) are quite consistent too. A complete confusion, however, exists about the equilibrium orientation of the dipoles, which is the most basic parameter for setting up any microscopic model. For RbBr: Ag^+ even the existence of the off-center position is still questionable, though the high-temperature electro-optical data[12] indicate alignable dipoles with small dipole moments.

It is the aim of this work to remove the uncertainties and to explain the inconsistencies among the results from previous work by a careful study of both the statics and dynamics of the low-temperature paraelectric behavior of RbCl: Ag^+ and RbBr: Ag^+. The method of electrodichroism, which has been most successfully used to determine equilibrium orientations and the statics and dynamics of the alignment of OH^- ions in alkali halides,[14–16] will be employed. In particular, the study of the peculiar reorientation kinetics will be of crucial importance to explain many of the previous inconsistencies.

II. EXPERIMENTAL TECHNIQUES

The single crystals were grown from ultrapure material (Merck) by the Kyropoulos technique under highly controlled conditions in an argon atmosphere,[17] with dopings of 0.1- to 1-mole% AgCl or AgBr added to the melt. Crystal slices of different orientations were cut and polished to the dimensions desired, the orientations being controlled afterwards by the Laue x-ray back-reflection technique. Before the measurements, the samples were heated to about 600 °C and quenched to room temperature to avoid silver aggregation. The Ag^+ concentration was determined by optical measurements, using the oscillator strength given in Ref. 4.

The optical measurements were performed in a variable-temperature He cryostat, the temperature

TABLE I. Conclusions and data about off-center behavior of Ag^+ in RbCl and RbBr, derived from previous work.

Method	Derived conclusions and data RbCl : Ag^+	RbBr : Ag^+
Temperature dependence of uv absorption strength[a]	Off-center position for $T < 120$ °K	Off-center position for $T < 140$ °K
Electrocaloric[b]	⟨111⟩ dipoles, $p = 0.85\ e$ Å	Negative
Point-ion-model calculation[c]	Off-center potential, ⟨111⟩ minima displaced by 0.54 Å	On-center potential
Far infrared[d]	⟨110⟩ dipoles, $p \sim 0.1\ e$ Å	Not investigated
Paraelectric resonance[e]	⟨111⟩ or ⟨110⟩ dipoles $p = 0.85\ e$ Å, $\Delta < 0.1$ cm^{-1}	Not investigated
Dielectric constant[f]	⟨111⟩ dipoles, $p = 1.0\ e$ Å	Not investigated
Elastic model[f]	⟨100⟩ elastic dipoles	Not investigated
uv electro-optic[g]	Not investigated	Dipoles close to ⟨110⟩, $p = 0.23\ e$ Å
Specific-heat anomaly[h]	Tunneling defects, $\Delta <$ strain splitting	Not investigated

[a]Reference 4. [b]Reference 5. [c]Reference 6. [d]Reference 9. [e]Reference 7. [f]Reference 10. [g]Reference 12. [h]Reference 11.

being monitored by a calibrated resistor glued to the crystal. The crystal holder was designed so that the light propagated parallel to the electric field through metal-net electrodes, supported by thin quartz plates. The optical measurements therefore always show the absorption in the plane perpendicular to the applied field. The only exception from this geometry is the measurement in Fig. 5, in which the electric field was applied perpendicular to the light propagation direction, while the absorption was measured again with light polarized perpendicular to the applied field. For this case only, the electric field was an ac field and the field-induced absorption changes were measured using phase-sensitive lock-in amplification of the photoelectric signal. The time dependence of the optical absorption after a quick change ($\sim 10^{-8}$ sec) of the applied field was followed either with a Cary 14 spectrometer or by oscillographic display of the photoelectric signal.

III. STATIC BEHAVIOR OF ELECTRODICHROISM

The upper part of Fig. 1 shows the uv absorption spectra of Ag^+ in RbCl and RbBr, which have been described previously in the literature.[2,12] The spectra of both crystal systems are very similar, consisting of a well-separated low-energy band ("A band"), two partially overlapping bands ("D_1" and "D_2") at higher energies (which are better separated in RbBr), and a subsequent band ("F") at still higher energies. In the lower part of Fig. 1 is plotted the measured spectral dependence of the field-induced absorption change ΔK for the same electric field applied in the ⟨100⟩, ⟨111⟩, and ⟨110⟩ directions. While for RbCl : Ag^+ the lowest possible temperature (1.8 °K) could be chosen, giving "instantaneous" absorption changes under field application, for RbBr : Ag^+ a higher temperature (5.25 °K) was necessary to obtain the steady state of ΔK in a reasonable length of time (about 3 min; see Sec. IV). The absorption changes ΔK were measured for ⟨100⟩ and ⟨111⟩ fields with unpolarized light in the plane perpendicular to the applied field, while for a [110] field the two inequivalent directions perpendicular to the field ($[1\bar{1}0]$ and [001]) were measured separately using a uv polarizer. All observed ΔK spectra consist—within the experimental accuracy and the uncertainty of the D_1/D_2 band separation—of pure zero-moment changes of the A, D_1, D_2, and F band. Direction and magnitude of these zero-moment changes are different for all four bands and vary strongly with the applied-field direction. The changes in the A_1, D_1, and D_2 bands look nearly identical for the two systems RbCl : Ag^+ and RbBr : Ag^+. The measured ΔK spectra in RbBrAg^+ agree qualitatively with the modulation spectra measured at high temperature by Sittig[12]; however, in his measurement the two inequivalent spectra observed perpendicular to the ⟨110⟩ field were not

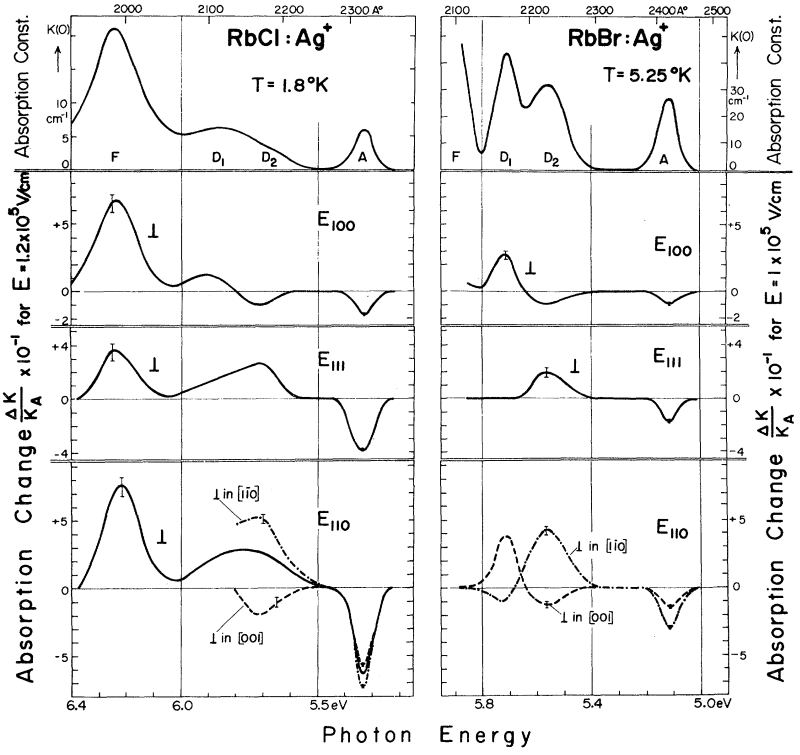

FIG. 1. Upper part: uv absorption spectrum of Ag^+ ions in RbCl and RbBr. (The Ag^+ doping was 1×10^{-3} and 2.5×10^{-3} in the melt for RbCl and RbBr, respectively.) From the optical density an Ag^+ concentration of 7×10^{-5} in the crystal is estimated for RbCl, using the calibration factor from Ref. 4. Lower part: Spectral dependence of the field-induced dichroism, measured with light polarized perpendicular to electric fields applied in the ⟨100⟩, ⟨111⟩, and ⟨110⟩ directions. (For RbCl:Ag^+, $T=1.8$ °K and $E=1.2\times10^5$ V/cm were used; and for RbBr:Ag^+, $T=5.25$ °K and $E=1\times10^5$ V/cm.) For fields applied in a [110] direction (lowest part) the dichroism was measured in both directions perpendicular to E separately, using a uv polarizer.

separated.

The following qualitative conclusions can be drawn from the ΔK spectra:

(i) The observed pure zero-moment changes indicate that the dichroism is predominantly caused by the *field-induced reorientation* of the optically anisotropic Ag^+ ions.

(ii) The existence of strong ΔK effects for all three field directions excludes a ⟨100⟩ or ⟨111⟩ dipole model, for which ⟨111⟩ or ⟨100⟩ fields, respectively, should not produce any reorientation dichroism. A ⟨110⟩ *dipole model* seems therefore most likely.

(iii) The observed decrease of the *A band* (measured perpendicular to E) for all field directions indicates a transition moment parallel to the electric dipole (σ *polarization*). The relative ΔK magnitudes are consistent with a ⟨110⟩ dipole model.

(iv) The direction and relative magnitude of the changes in the D_1 *and* D_2 *band* are consistent with their assignment to the two inequivalent π *polarized* transitions perpendicular to the ⟨110⟩ dipole, with the D_1 band being π_{001} polarized and the D_2 band $\pi_{1\bar{1}0}$ polarized.

The model for our qualitative interpretation is illustrated in Fig. 2, showing the classical ⟨110⟩ dipoles with their 12 equivalent orientations. Electric fields of different directions split the twelvefold-degenerate ground state in the indicated way, leading to a Boltzmann equilibrium population of the split levels. The anisotropic optical absorption of each dipole can be described by transition moments parallel (σ) and perpendicular (π_{001} and $\pi_{1\bar{1}0}$) to the

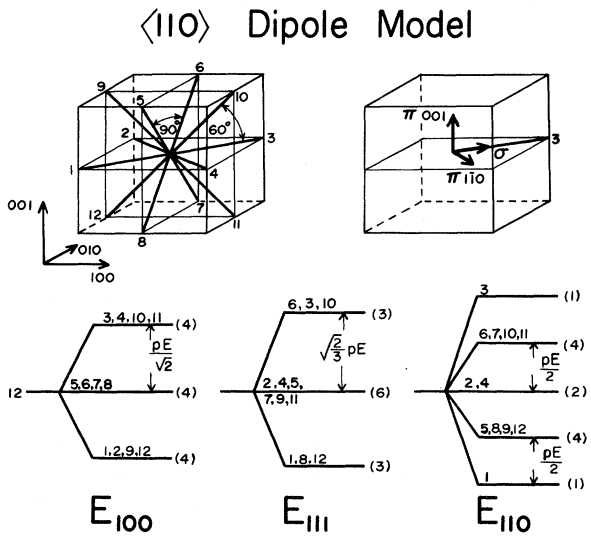

FIG. 2. Illustration for the 12 equivalent sites of a ⟨110⟩ dipole and the three directions (σ, π_{001}, and $\pi_{1\bar{1}0}$) for the optical transition moments of a single dipole (upper part). Below are sketched the (classical) energy levels for the orientational states of ⟨110⟩ dipoles under an applied ⟨100⟩, ⟨111⟩, and ⟨110⟩ field, with indication of splitting energy and level multiplicity.

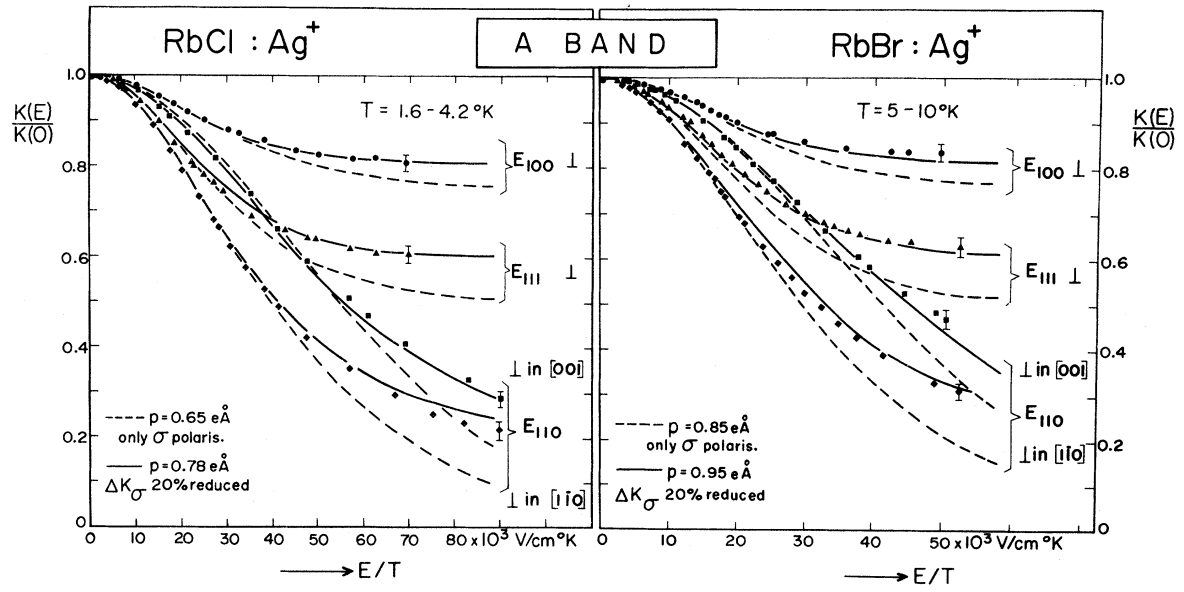

FIG. 3. Relative absorption change $K(E)/K(0)$ in the peak of the A band, under applied fields in ⟨100⟩, ⟨111⟩, and ⟨110⟩ directions, plotted against E/T. The measurements were performed between 1.6 and 4.2 °K for RbCl : Ag$^+$ and between 5 and 10 °K for RbBr : Ag$^+$. Calculated curves (dotted and full lines) based on a ⟨110⟩ dipole model, were fitted to the experimental points, using a one-parameter and a two-parameter fitting model, as discussed in the text.

dipole axis, as sketched in the upper right-hand side of Fig. 2. Reorientation of the dipoles, i.e., of the transition moments, causes the dichroism.

For a quantitative test of this model, the field-induced changes in the maximum of the A band were measured as a function of variable ⟨100⟩, ⟨111⟩, and ⟨110⟩ fields for both crystal systems (Fig. 3). The data were taken under variation of the temperature as indicated in the figure. Plotted against E/T, they yield a coinciding behavior for each field direction, with the ⟨110⟩ field again producing two different effects in the two inequivalent directions perpendicular to E. Using the ⟨110⟩ paraelectric model sketched in Fig. 2, the expected E/T dependence of an absorption with pure σ polarization was calculated. With the electric-dipole moment p as the only fitting parameter, a good fit to all four curves can be obtained for both crystal systems in the low E/T range (dotted curves). For large E/T values, however, these calculated curves deviate systematically from the measurements, predicting too large $|\Delta K(E)|$ absorption changes. A perfect fit over the whole measured E/T range can be obtained for both crystal systems, if we allow a 20% reduction of all calculated $|\Delta K(E)|$ values and use the dipole-moment values 0.78 and 0.95 e Å for RbCl : Ag$^+$ and RbCl : Ag$^+$, respectively, as fitting parameter (full curves in Fig. 3).

Similar, but less-detailed, measurements have been performed on the absorption change of the relatively well-separated D_1 and D_2 band in RbBr : Ag$^+$ (Fig. 4). Again the expected behavior was calculated

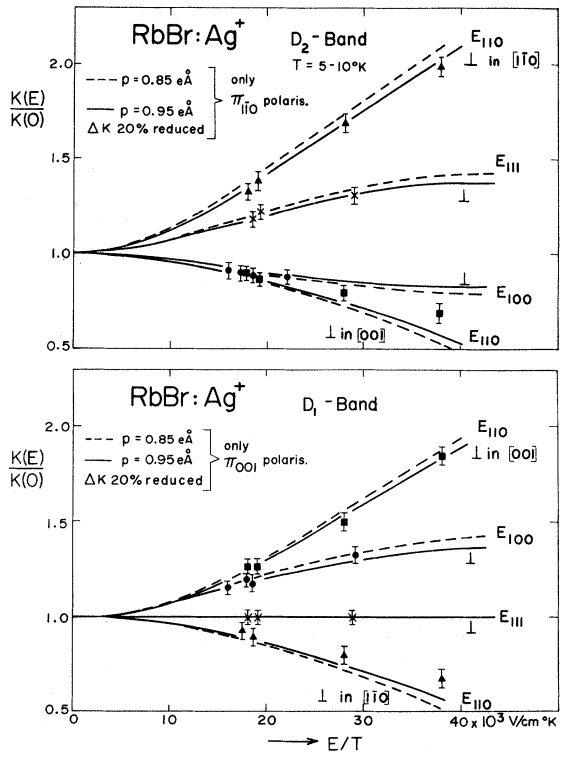

FIG. 4. Relative absorption change $K(E)/K(0)$ of the D_2 and D_1 band in RbBr : Ag$^+$ measured between 5 and 10 °K under ⟨100⟩, ⟨111⟩, and ⟨110⟩ applied fields with perpendicular polarized light, plotted against E/T. The full and dotted lines are calculated curves using the two fitting models described in the text.

for ⟨110⟩ dipoles, assuming full π_{001} polarization for the D_1 band and $\pi_{1\bar{1}0}$ polarization for the D_2 band. Both fitting models used in Fig. 3 ($p = 0.85\ e$ Å, and $p = 0.95\ e$ Å with 20%-reduced $|\Delta K|$ values) lead to an equal good fit to the measurements in the covered E/T range.

In conclusion, we can state the following: The electrodichroism of the A, D_1 and D_2 band and its dependence on field direction and strength and on temperature can be quantitatively explained by a paraelectric ⟨110⟩ off-center dipole model for Ag^+ in both RbCl and RbBr. Using the most simple (one-parameter) model, which assumes full σ, π_{001}, and $\pi_{1\bar{1}0}$ polarization for the A, D_1 and D_2 bands, respectively, a good fit to all curves can be obtained in the low E/T range, yielding dipole-moment values of 0.65 and 0.85 e Å for RbCl and RbBr, respectively. This simple model, however, shows systematic deviation from the measurements in the high E/T range (Fig. 3) so that a second parameter must be introduced into the model. By the introduction of a 20% reduction for all $|\Delta K(E)|$ values in all three bands, a quantitative fit to all measured curves over the whole E/T range can be obtained using a single-dipole-moment value as fitting parameter (0.78 and 0.95 e Å for Ag^+ in RbCl and RbBr, respectively). In order to explain this $|\Delta K|$ reduction, we have to relax one of the three rigid conditions used so far for our model, namely, (a) that all optically detected Ag^+ ions are equally alignable; (b) that the A, D_1 and D_2 bands are purely σ, π_{001}, and $\pi_{1\bar{1}0}$ polarized; (c) that the dipoles are rigidly oriented in ⟨110⟩ directions. This leads to three possibilities for the explanation of the $|\Delta K|$ reduction:

(i) 20% of the optically detected Ag^+ ions do not participate in the alignment process. This could be due to interaction effects among the Ag^+ ions, so that the $|\Delta K|$ reduction would be expected to be concentration dependent.

(ii) An admixture of 8% π absorption for the σ-polarized A-band transition, and vice versa an 8% admixture of σ absorption to both π-polarized transitions (D_1 and D_2 band) would explain quantitatively the $|\Delta K|$ reduction. A physical reason for such a particular optical anisotropy is, however, not clear.

(iii) Small angular deviations from the exact ⟨110⟩ orientation due to librational motion of the dipoles can be the origin of the $|\Delta K|$ reduction. The 20% value of $|\Delta K|$ reduction would be produced by a mean angular zero-point displacement of 16° from the exact ⟨110⟩ orientation. From the three possible explanations the last one appears most likely and physically attractive. If this last interpretation (iii) holds, the observed $|\Delta K|$ reduction becomes an important quantity of the model, being directly related to the amplitude of the zero-point libration of the Ag^+ dipole.

For the high-energy F band, no detailed field-dependence measurements of the type in Figs. 3 and 4 were performed. The observed electrodichroism values of Fig. 1 ($\Delta K/K = +0.17$, $+0.09$, and $+0.20$ for fields in ⟨100⟩, ⟨111⟩, and ⟨110⟩, respectively) can, however, be interpreted within our derived model. Using the dipole-moment parameter and 20% $|\Delta K|$ reduction, derived from the electrodichroism of the low-energy bands, we obtain the best fit to the measured $\Delta K/K$ values of the F band, by assuming a 3 : 1 mixture of π_{001} and $\pi_{1\bar{1}0}$ polarization for the F-band transition moment. This yields a calculated dichroism of $+0.16$, $+0.07$, and $+0.21$ for fields in ⟨100⟩, ⟨111⟩, and ⟨110⟩ directions, in good agreement with the above-mentioned experimental data. The marked difference in the polarization of the F band compared to the three low-energy bands is consistent with their different interpretation. The A, D_1 and D_2 bands are in general interpreted as an internal $4d^{10} \rightarrow 4d^9 5s$ transition of the Ag^+ ion and thus reflect in their polarization the C_{2v} symmetry of the Ag^+ ⟨110⟩ off-center position. The F band, however, is regarded as a (parity-forbidden) charge-transfer transition, the polarization of which would be determined both by the Ag^+ off-center ion and the arrangement of the surrounding lattice ions, to which the charge transfer occurs.

From the temperature dependence of the absorption strength, it was concluded[12] that the off-center properties would change strongly with temperature and that eventually the potential for the Ag^+ should become centrosymmetric (at about 120 °K for RbCl, and at somewhat higher temperature for RbBr). The electrodichroism can be used as sensitive method to check this out. As long as paraelectric off-center properties with *constant dipole moment* p prevail, the electrodichroism should follow a $(pE/kT)^2$ dependence. Figure 5 shows the results for RbCl and RbBr obtained by ac field modulation of the A band, detected with lock-in techniques. For RbBr : Ag^+, a T^{-2} dependence was observed up to ~ 200 °K, demonstrating clearly off-center behavior with constant displacement dipole up to this temperature. For RbCl : Ag^+, however, the initial low-temperature T^{-2} dependence changes above 15 °K into a stronger ($\sim T^{-3.3}$) temperature dependence. This could, in fact, be due to temperature-induced changes of the off-center potential, as assumed in Ref. 12. It could, however, be explained too, within a temperature-independent potential model, by a gradual thermal population of the vibrational levels of the off-center potential. The potential for the radial displacement of the Ag^+ is expected to be strongly anharmonic, so that in the excited radial vibrational states (21 or 26 cm^{-1}; in Ref. 9) the Ag^+ ion could have a smaller dis-

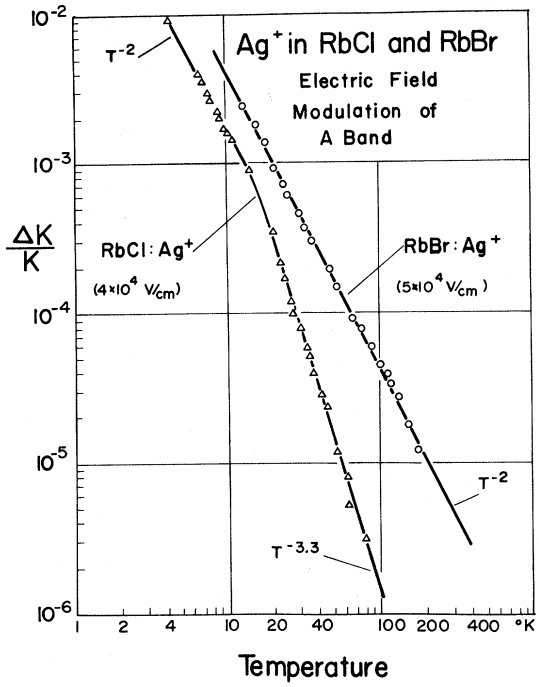

FIG. 5. Temperature variation of the electric field modulation of the A band in RbCl: Ag^+ and RbBr: Ag^+. For this case only, an ac electric field $E(110)$ was applied perpendicular to the propagation direction of the light. The absorption changes $|\Delta K/K|$ were measured with light polarized perpendicular to E in $[1\bar{1}0]$, using phase-sensitive lock-in detection. The plotted $|\Delta K/K|$ are uncorrected values measured relatively to a full modulation of the transmitted light by a chopper.

placement from the center, i.e., a smaller dipole moment. Increasing thermal population of these levels could, therefore, cause the extra T dependence in Fig. 5.

IV. DYNAMIC BEHAVIOR OF ELECTRODICHROISM

After clarification of the Ag^+ static paraelectric properties under constant electric fields, we will now attempt to determine the *dynamic* alignment properties of the defect. A knowledge of the dipole-lattice relaxation behavior is of great importance, as it supplies a direct measure of the coupling strength between the defect and host lattice, and allows conclusions about the tunneling splitting by applying theoretical models.[18] While some measurements of the dipole-lattice relaxation time have been performed previously in RbCl: Ag^+ using electrocaloric[5] and dielectric-loss measurements,[10] no low-temperature measurements are available for RbBr: Ag^+ so far.

More detailed information, compared to the above-mentioned two techniques, can be obtained on the dipole-lattice relaxation behavior by monitoring the electrodichroism after a rapid change of the applied electric field. In contrast to the "integral" nature of dielectric and electrocaloric measurements, this method is "defect specific" (as it monitors only the well-characterized optical absorption of the defect in question) and allows moreover to follow in detail the time dependence of the relaxation process (detecting, e.g., deviations from a single-exponential behavior). The method has been successfully applied to ⟨100⟩-oriented OH^- dipoles, for which it established the predominance of 90° reorientation, and determined the temperature regions of one-phonon and multiphonon relaxation.[15]

For our measurements, the well-separated A band, which lies in the most convenient spectral range, was used. A ⟨100⟩-, ⟨111⟩-, or ⟨110⟩-oriented electric field of about 1×10^5 V/cm was switched on $(0\rightarrow E)$, changed in polarity $(+E\rightarrow -E)$, and switched off $(E\rightarrow 0)$, each switching process being performed with a time constant of $\sim 10^{-8}$ sec (see lower part of Fig. 6). The time dependence of the A-band absorption (measured perpendicular to E) was monitored after each switching process. The obtained results are summarized in Fig. 6. For ⟨111⟩ fields (upper-part) the field application is followed by an absorption decrease with a time constant of $\tau\sim 0.1$ sec. Inversion of the field polarity causes a transient absorption increase and subsequent decrease with a similar time constant, while field removal causes increase of the absorption to its original $K(0)$ value with a time constant somewhat smaller than 0.1 sec. Under ⟨100⟩ fields the behavior is found to be completely different (middle part in Fig. 6): For $(0\rightarrow E)$ and $(E\rightarrow 0)$ the absorption decreases, respectively, increases with a time constant of about 100 sec, while for $(+E\rightarrow -E)$ no transient effect appears. Quantitatively the same behavior is found for ⟨110⟩ fields if the absorption was monitored in the [001] direction perpendicular to E_{110}. Measuring, however, for the ⟨110⟩ field in the other direction ($[1\bar{1}0]$) perpendicular to E, a completely different behavior is found (lower part in Fig. 6). For $(0\rightarrow E)$ an initial rapid absorption decrease (not resolved in Fig. 6) with a time constant of about 0.1 sec is followed by a slow ($\tau\sim 100$ sec) decrease. Under field inversion a rapid transient increase and subsequent decrease ($\tau\approx 0.1$ sec, resolved in the insert) appears. After field removal, a large rapid ($\tau\approx 0.1$ sec) absorption increase "overshoots" the $K(0)$ value and is followed by a slow decay ($\tau\approx 100$ sec) towards $K(0)$. In summary, there appear *two relaxation processes with three orders-of-magnitude different time constants*, the relative magnitude of which vary strongly with the field direction.

For interpretation of this complex behavior, one has to realize that ⟨110⟩ dipoles can reorient among their 12 equivalent orientations (see Fig. 2) via

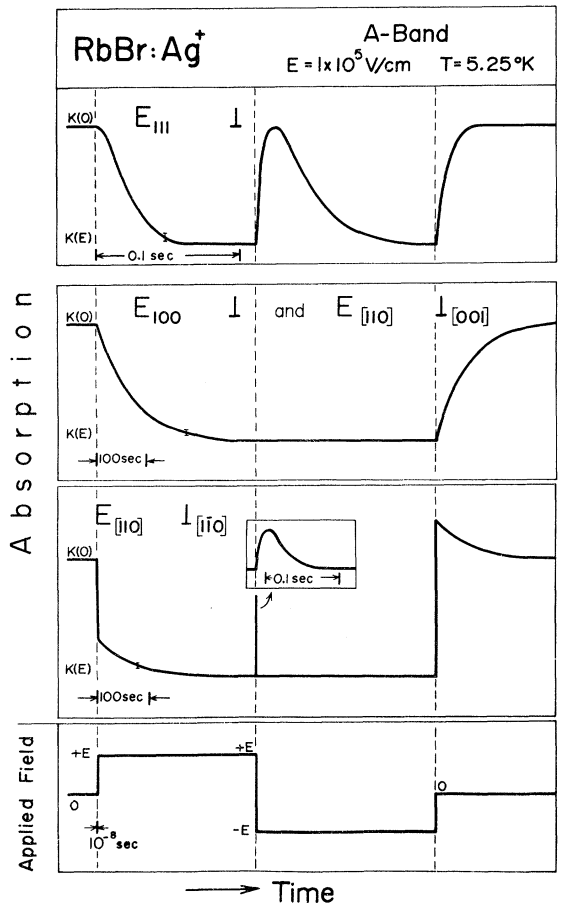

FIG. 6. Time dependence of the A band electrodichroism measured for three switching operations ($0 \rightarrow E$, $+E \rightarrow -E$, $E \rightarrow 0$, see lower part) of an electric field (1×10^5 V/cm) applied in ⟨111⟩, ⟨110⟩, and ⟨100⟩ directions. The light is polarized perpendicular to E; for E_{110} the two different perpendicular directions are measured separately. Note the different time scales in the different parts and in the insert.

60° or 90° rotations (nearest-neighbor or next-nearest-neighbor reorientation). We illustrate in the left-hand side of the level diagrams in Fig. 7 how the dipole levels, split by ⟨111⟩, ⟨100⟩, and ⟨110⟩ fields, are connected by 60° or 90° reorientation processes. The result, easily verified by geometrical inspection of Fig. 2, is the following:

(a) 60° reorientation processes can achieve full relaxation among all dipole levels in all three cases.

(b) 90° reorientation processes achieve relaxation only among the four dipoles lying in a common {100} plane (see Fig. 2). The 90° process alone will, therefore, in most cases, not achieve full dipole relaxation.

At first sight, nearest-neighbor (60°) reorientation would appear to be much more likely than 90° reorientation. This was indeed found for the ⟨110⟩-oriented O_2^--elastic-dipole defects by Känzig and co-workers,[19] and it was subsequently argued that from general considerations 60° reorientation should always exceed the 90° process.[20] If we assume this to hold in our case too, we would expect a very similar relaxation time for ⟨100⟩, ⟨111⟩, and ⟨110⟩ fields, because in all cases full relaxation could be achieved by the predominant 60° process. The measurements in Fig. 6, however, are definitely in disagreement with this.

We, therefore, attempt the alternative assumption, namely, that 90° reorientation is strongly predominant over the 60° process. For this case, the dipoles will relax via 90° reorientation wherever possible and will reorient by 60° rotation only when the 90° process cannot achieve full relaxation. The strong arrows at the right-hand side of the level diagrams in Fig. 7 show the actual relaxation transitions for this case: a mixture of 90° and 60° transitions for ⟨100⟩ and ⟨110⟩ fields; pure 90° transitions, however, for ⟨111⟩ fields. From this model we can first of all predict the relative amount of energy dissipated after application of a

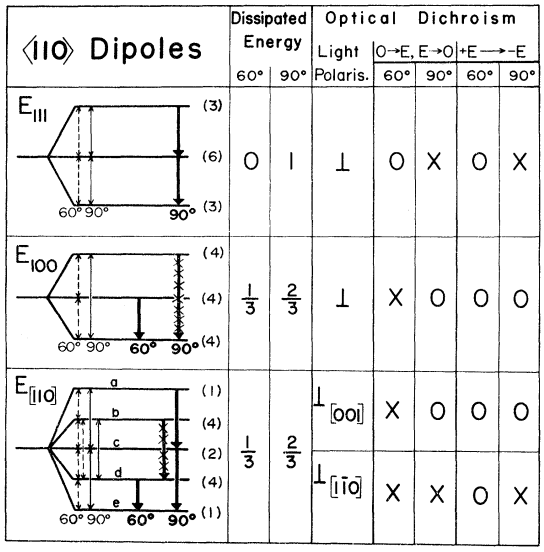

FIG. 7. Relaxation model for the ⟨110⟩ Ag^+ dipoles, assuming predominant 90° reorientation processes. The level diagrams (for three field directions) show on the left-hand side (thin arrows) the general possibilities for 60° and 90° transitions, while on the right-hand side the actually chosen relaxation transitions (after field application) are indicated by strong arrows. The "optically invisible transitions" are marked by crosses. On the left-hand side of the adjoining table is indicated the relative amount of energy, dissipated by 60° and 90° relaxation processes under a saturation field. On the right-hand side are listed the expectations for observing (X) and nonobserving (0) of 60° and 90° relaxation in the optical dichroism under the three switching operations ($0 \rightarrow E$), ($E \rightarrow 0$), and ($+E \rightarrow -E$).

saturation electric field in the relaxation process via the rapid 90° and slow 60° process (first columns in table of Fig. 7). Moreover, we can predict what type of optical-absorption changes we expect to see for each applied-field direction after the three switching operations. To figure that out, we have to realize that dipoles which exchange their energy levels under field inversion are "optically indistinguishable," so that direct transitions between these dipole states do not appear as absorption changes. We have, therefore, crossed out these transitions in the level diagrams of Fig. 6, marking them as "optically invisible." From the remaining "optically visible" transitions the following expectation can be directly derived, as illustrated and tabulated in Fig. 7:

a. ⟨111⟩ *field*. We expect rapid 90° relaxation processes for $(0 \rightarrow E$ and $E \rightarrow 0)$. Under field inversion the system relaxes by 90° transitions through the middle level, so that a temporary rapid absorption change is expected.

b. ⟨100⟩ *field*. The middle level is connected to the outer levels only by a slow (60°) optically visible transition. We, therefore, expect slow absorption decreases and increases for $(0 \rightarrow E)$ and $(E \rightarrow 0)$. Relaxation after field inversion can be achieved by the direct (optically invisible) 90° transition between the outer levels; therefore, no transient absorption change is expected.

c. ⟨110⟩ *field*. (i) For [001] polarization, we see in optical absorption only the dipoles in the two (optically indistinguishable) levels b and d, which are coupled by a quick 90° process to each other, but coupled to the other dipole levels a, c, e by a slow 60° process only. Consequently, we expect a slow absorption decrease and increase under $(0 \rightarrow E)$ and $(E \rightarrow 0)$, but no transient absorption effect, however, under field inversion. Thus the expected behavior is identical to the case of the ⟨100⟩ field.

(ii) For $[1\bar{1}0]$ polarization, we optically detect the dipoles in level c with full absorption strength, and the dipoles in levels b and d with 0.25 absorption strength. After field application we expect to see the depopulation of level c via a rapid 90° process and the slow depopulation of level d by 60° relaxation. After field inversion, a quick transient absorption increase should appear, due to the temporary filling of level c during the (90°) $e \rightarrow c \rightarrow a$ relaxation. Under field removal initially the levels a, c, and e (connected by rapid 90° processes) will relax, which will temporarily put more dipoles in level c than under $E = 0$ equilibrium. As the dipoles in level c absorb most strongly, we therefore expect a rapid absorption increase after $(E \rightarrow 0)$ to a K value larger than $K(0)$. In the subsequent slow 60° relaxation process between multiplet (a, c, e) and (b, d), this "overshooted" absorption is expected to decay slowly to the equilibrium value $K(0)$.

We recognize that these detailed predictions of our model, summarized in Fig. 7, account qualitatively for the complex relaxation behavior of the electrodichroism for all cases of field and polarization direction and switching operation (Fig. 6). This agreement extends into all details, and can be checked and analyzed quantitatively by setting up the equations for the relaxation kinetics of the three systems in Fig. 7. We show this explicitly for the ⟨111⟩ field case, in which the three levels are connected by 90° relaxation processes with a transition rate $w(\Delta U)$, where $\Delta U = \sqrt{\frac{2}{3}} pE$. Using $w \equiv w_{\text{absorption}} = w_{\text{emission}}\, e^{-\Delta U/kT}$, we can give the kinetic equations for the population in the three levels (numbered 1, 2, 3 in order of increasing energy):

$$\begin{aligned} \dot{n}_1 &= -2wn_1 + wbn_2 \,, \\ \dot{n}_2 &= -w(1+b)n_2 + 2wbn_3 + 2wn_1 \,, \\ \dot{n}_3 &= -2wbn_3 + wn_2 \,, \end{aligned} \tag{1}$$

with $b = e^{\Delta U/kT}$. Following the procedure in Refs. 16 and 18, we choose two new variables and express them by their deviations from the equilibrium value (denoted by a bar):

$$\begin{aligned} x &\equiv \bar{x} + \Delta x = n_1 - n_3 \equiv (\bar{n}_1 - \bar{n}_3) + \Delta(n_1 - n_3) \,, \\ y &\equiv \bar{y} + \Delta y = n_1 + n_3 \equiv (\bar{n}_1 + \bar{n}_3) + \Delta(n_1 + n_3) \,. \end{aligned} \tag{2}$$

In terms of these quantities, the relaxation of the system after quick change to a new (time-independent) field value becomes

$$\begin{aligned} \Delta\dot{x} &= -w(b+1)\Delta x \,, \\ \Delta\dot{y} &= -2w(b+1)\Delta y + w(b-1)\Delta x \,. \end{aligned} \tag{3}$$

We realize that the quantity $x = n_1 - n_3$ is proportional to the *electric polarization*, while $y = n_1 + n_3$ is proportional to the *optical absorption* of the system.

After field switching $(E \rightarrow 0)$, the system relaxes under zero field, i.e., at $b = 1$, so that we expect

$$\Delta\dot{x} = -2\omega\Delta x, \quad \Delta\dot{y} = -4\omega\Delta y \,, \tag{4}$$

i.e., a simple-exponential relaxation behavior of both electric polarization and optical absorption. The experimentally determined relaxation times of the optical dichroism (τ_{opt}) and of the electric polarization (τ_{pol}) should therefore be

$$\tau_{\text{opt}}(E_{111} \rightarrow 0) = \tfrac{1}{2}\tau_{\text{pol}} = 1/4w \,. \tag{5}$$

After the switching on of the field $(0 \rightarrow E)$, the system relaxes under a constant value b. Equation (3) then yields the solution

$$\Delta y(t) = \Delta y(0)\,(2e^{-(b+1)wt} - e^{-(b+1)2wt}) \,. \tag{6}$$

This equation described exactly the measured time-dependence curve in Fig. 6 for $(0 \rightarrow E_{111})$. It starts out horizontally, because initially the depopulation

of the upper level at $t=0$ is equal to the population increase of the lowest level, so that $n_1+n_3=$ constant. We characterize this nonexponential relaxation behavior of the optical dichroism again formally by the $1/e$ point of the measured curve, which yields an experimental decay-time parameter τ. Solving Eq. (6) for this $1/e$ value, we obtain

$$\Delta y(t)/\Delta y(0)=e^{-1}\approx 2e^{-1.6}-e^{-3.2}\ , \tag{7}$$

which yields

$$\tau_{\rm opt}(0\rightarrow E_{111})=1.6/(b+1)w \tag{8}$$

or, for small fields ($b\approx 1$),

$$\tau_{\rm opt}(0\rightarrow E_{111})=0.8/w=3.2\tau_{\rm opt}(E_{111}\rightarrow 0)\ . \tag{9}$$

In similar ways the kinetic equations for the relaxation under ⟨100⟩ and ⟨110⟩ fields can be set up, and all relations between the experimental decay times of the optical dichroism and the electric polarization and the 90° and 60° transition rates (w and v, respectively) can be derived. For the ⟨100⟩ *field case*, we obtain, e.g., a relation of the optically observed decay times to the 60° transition rate v for small fields ($b\approx 1$),

$$\tau_{\rm opt}(0\rightarrow E_{100})=\tau_{\rm opt}(E_{100}\rightarrow 0)=1/6v\ . \tag{10}$$

For this case the relaxation of the electric polarization should show both a rapid and slow process, with relaxation times at small fields ($b\approx 1$)

$$\begin{aligned}&\tau_{\rm pol}(60^\circ)=1/2v=3\tau_{\rm opt}(E_{100})\ ,\\ &\tau_{\rm pol}(90^\circ)=1/2w\ .\end{aligned} \tag{11}$$

The quantitative treatment of the [110] *field case* is somewhat more complicated due to the presence of five levels (a, b, c, d, e in Fig. 7). In our optical experiment, however, we detect for [001] polarization only the levels b and d, while for $[1\bar{1}0]$ polarization level c (and additionally, with one-quarter strength, levels b and d again) is detected. Thus the optically detected relaxation phenomena can be related to the calculated kinetic equations for the relaxation of the quantities (n_b+n_d) and n_c. This leads, for (n_b+n_d), to the same equations as the relaxation of the optical dichroism under ⟨100⟩ fields.

It is evident from our discussion that the Ag^+ system offers a possibility which is unique among all paraelectric defects studied so far. We can measure the reorientation process through each of the two possible reorientation angles (60° and 90°) separately and can thus determine their individual temperature dependence. In Fig. 8, we summarize the results of a large set of experiments in which the time-dependence of the A-band electrodichroism after $(0\rightarrow E)$ and $(E\rightarrow 0)$ switching of a ⟨100⟩, ⟨111⟩, and ⟨110⟩ field was measured for both systems RbCl: Ag^+ and RbBr: Ag^+ as a function of temperature. Each point in Fig. 8 was obtained from a time-dependent absorption curve (like in Fig. 6) by taking the time value at which the absorption had decreased (or increased) by a fraction $1/e$ of the total $|\Delta K|$. These experimental "optical relaxation times" were plotted logarithmically in Fig. 8 in two ways: against $\ln T$ and against $1/T$. During the temperature variation, the electric field was adjusted so that pE/kT (or in other words the static value of the electrodichroism) was kept about constant.

The behavior analyzed for RbBr: Ag^+ at a single temperature (Fig. 6) is found to extend for this system over the whole measured temperature range. Moreover, the same type of behavior is found now for the RbCl: Ag^+ system too: a slow relaxation process under ⟨100⟩ fields, a rapid relaxation process under ⟨111⟩ fields, and for ⟨110⟩ fields a superposition of the slow and rapid process. Thus, our model summarized in Fig. 7 holds for both crystals, and we can, therefore, mark for both systems the rapid process as "90° reorientation" and the slow one as "60° reorientation."

In Fig. 9 we show how the optically determined relaxation times measured for $(0\rightarrow E_{111})$ and $(E_{111}\rightarrow 0)$ at different temperatures depend on the field strength (i.e., splitting of the levels). For each temperature, the $\tau_{\rm off}$ and $\tau_{\rm on}$ values were normalized to the $\tau_{\rm off}(E\approx 0)$ value, obtained for the same temperature. By this normalization, the temperature dependence of $\tau(E\approx 0)$ is eliminated. We first recognize that the relaxation under zero field ($\tau_{\rm off}$) is completely independent of the original field splitting, as expected. The value of $\tau_{\rm on}$ is found to be (for small fields $E<kT/p$) a factor of 3.2 higher than $\tau_{\rm off}$, as we expect from our kinetic equations (6)–(9). With increasing electric field (measured in units of pE/kT), the value of $\tau_{\rm on}$ decrease strongly at all temperatures. Note that at $pE/kT\approx 2.0$ (which we used for the measurements of RbBr: Ag^+ in Fig. 8) we have $\tau_{\rm on}\approx 2.8\tau_{\rm off}$, which accounts for the observed difference of the two quantities in Fig. 8.

To explain the observed field dependence of $\tau(0\rightarrow E_{111})$ in Fig. 9, we consider two relaxation mechanisms:

a. One-phonon-assisted tunneling. Using the relation between our experimental $\tau_{\rm opt}$ value and the transition rate w [Eqs. (8) and (5)], and the expression for the one-phonon transition probability,[18] $w(\Delta U)\propto \Delta U(e^{\Delta U/kT}-1)^{-1}$, we obtain

$$\frac{\tau_{\rm opt}(\Delta U)}{\tau_{\rm opt}(0)}=\frac{6.4}{b+1}\,\frac{w(0)}{w(\Delta U)}=\frac{e^{\Delta U/kT}-1}{e^{\Delta U/kT}+1}\,\frac{2kT}{\Delta U}\,3.2\ , \tag{12}$$

which is plotted as a function of pE/kT by the full line in Fig. 9 (using $\Delta U=\sqrt{\frac{2}{3}}\,pE$ and our dipole-moment value $p=0.95\,e$ Å).

b. Classical-rate process. For thermally

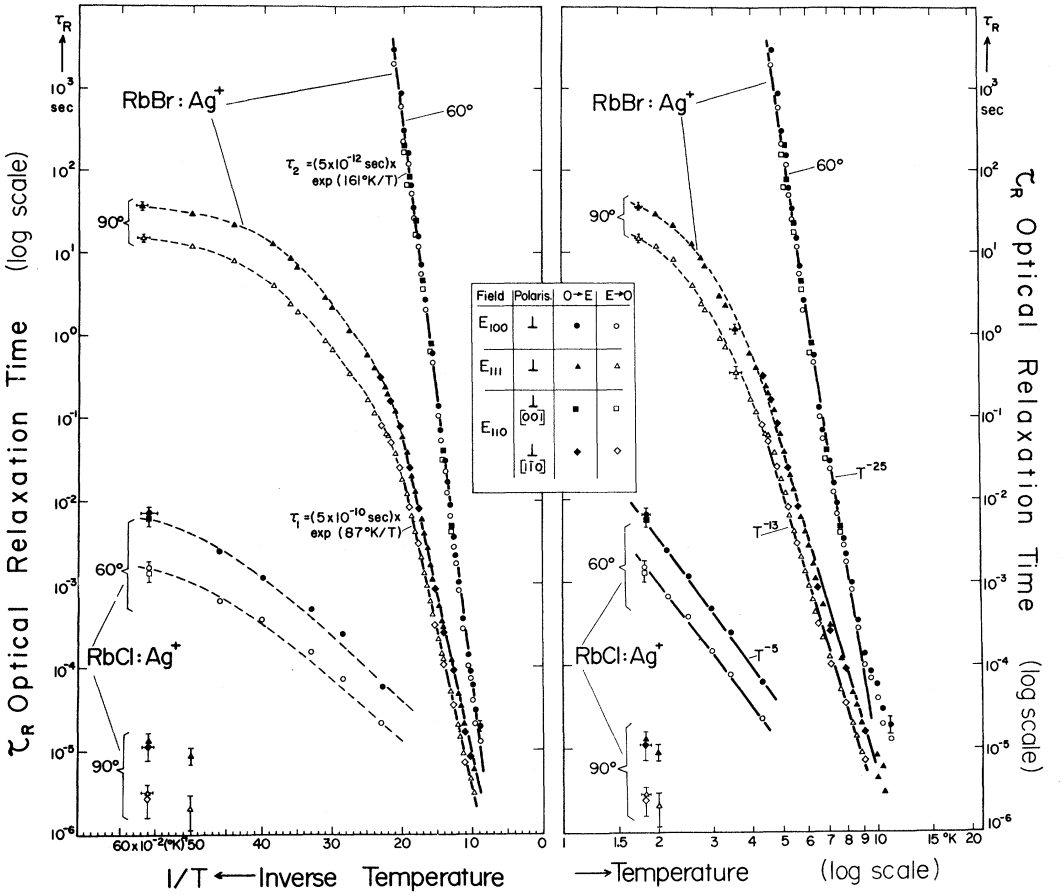

FIG. 8. Optical relaxation time of Ag^+ in RbBr and RbCl measured for different field directions and switching operations, as indicated, as a function of temperature, plotted logarithmically against $1/T$ (left-hand side) and against $\ln T$ (right-hand side). During temperature variation, the electric field strength was adjusted to keep approximately a constant Boltzmann factor over the whole range ($pE/kT = 2.0 \pm 0.05$ for RbBr and $pE/kT = 3.0 \pm 0.7$ for RbCl).

activated reorientation over a barrier $\Delta\epsilon$, we have the reorientation rate

$$\omega(\Delta U) = \text{const}\times e^{-(\Delta\epsilon+\Delta U/2)/kT} = w(0)e^{(-\Delta U/2kT)}. \quad (13)$$

This yields for Eqs. (8) and (9),

$$\frac{\tau(\Delta U)}{\tau(0)} = \frac{6.4}{b+1}\,\frac{w(0)}{w(\Delta U)} = 6.4[\,e^{\Delta U/2kT} + e^{-\Delta U/2kT}]^{-1}, \quad (14)$$

which is plotted as a dotted line in Fig. 9.

How can we explain the relaxation mechanism of the Ag^+ ion in terms of the measured field and temperature dependence of the relaxation time? First, we can state that the general temperature behavior of the relaxation—strong exponential dependence at high temperatures changing into a weak dependence at low temperatures—definitely suggests tunneling as the low-temperature reorientation mechanism. The detailed temperature dependence, however, is different from the one found and expected for other tunneling defects (which have a low-temperature T^{-1} dependence in the one-phonon range, and a T^{-4} dependence in the multiphonon-assisted tunneling range).[15,21] Both the RbCl: Ag^+ and RbBr: Ag^+ system display at the lowest temperatures a stronger than T^{-1} dependence (T^{-5} and $T^{-2.5}$, respectively). This could indicate that we are still in the multiphonon relaxation range and that the one-phonon range starts out at even lower temperatures than measured here. On the other hand, it is known from electrocaloric[22] and dielectric[23] measurements that interaction effects between paraelectric centers can seriously affect the temperature dependence of the relaxation in the one-phonon range, producing a dependence stronger than T^{-1}. The Ag^+ ions, in particular, have a tendency to aggregate together (which one tries to prevent by the quenching process). We, therefore, tentatively interpret the low-temperature ($T < 5$ °K) relaxation as a one-phonon-assisted tunneling process, modified by interaction effects. This is supported by the field dependence of τ (Fig. 9), which is found to be up to about 5 °K in

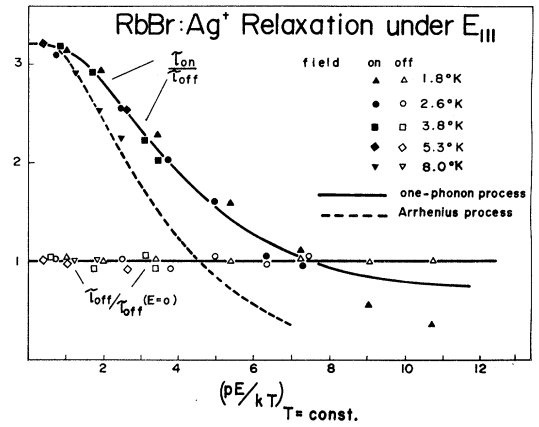

FIG. 9. Electric field dependence of the rapid 90° relaxation process of Ag^+ ions in RbBr, measured with ⟨111⟩ fields at various temperatures. The optical relaxation time for $0 \rightarrow E$ ("τ_{on}") and $E \rightarrow 0$ ("τ_{off}") are plotted in a normalized way as a function of electric field, which is measured for each temperature in units of (pE/kT). The $\tau_{off}(E)$ and $\tau_{on}(E)$ values were normalized to the low-field value $\tau_{off}(E \approx 0)$, obtained at the same temperature. The full line is calculated for one-phonon relaxation, the dotted line for a thermally activated rate process.

good agreement with the calculated behavior for one-phonon-assisted relaxation.

For $T > 5$ °K, a much stronger temperature dependence takes over (for RbBr : Ag^+), which can be described either by a very high negative power law in T or by an exponential process in T^{-1} (Fig. 8). While the high-power T dependence seems not to have any known physical significance, the Arrhenius law gives for both 60° and 90° reorientation reasonable attempt frequencies and activation energy values, which are consistent with considered barrier heights for the off-center Ag^+. Moreover, the relaxation time at 8° in this exponential range shows an E dependence in agreement with the calculated behavior for thermally activated classical reorientation (Fig. 9).

Sittig[12] has argued that the off-center potential should become less pronounced towards higher temperatures and become centrosymmetric at about 120–140 °K. A gradual decrease of the barrier height and off-center displacement with temperature could, of course, easily explain the exponential increase of the relaxation rate in Fig. 8. To check this possibility, we performed the measurement in Fig. 5. Its result clearly shows that the paraelectric alignment of the Ag^+ in RbBr follows a Curie law up to ~ 200 °K, demonstrating a temperature-independent displacement dipole. This most probably excludes that part of the T dependence of τ (below 10 °K) could be caused by a temperature dependence of the off-center potential.

One basic difference of the Ag^+ center to other paraelectric defects (like OH^-, Li^+) is its large mass ($m = 107$) which may seem to preclude sizable tunneling motion. It is instructive to compare it to a small mass defect like OH^-, for which basically the proton is the tunneling entity. The barrier height $\Delta\epsilon$ for the 90° reorientation of RbBr : Ag^+ (from the results in Fig. 8) is 60 cm^{-1} which is about an order of magnitude less than for OH^- ions. On the other hand, the librational frequency of Ag^+ ions is with $\hbar\omega \approx 25$ cm^{-1} again about one order of magnitude less than for OH^- ions. As for the harmonic-oscillator double-well holds $\omega_{tunnel} \propto e^{-2\Delta\epsilon/\hbar\omega}$, we expect very roughly comparable tunneling properties for both systems. On the other hand, it is evident from the $\Delta\epsilon$ and $\hbar\omega$ parameters of the two systems that thermally activated reorientation should become dominant at much lower temperatures for the Ag^+ compared to the OH^- system.

The most basic and interesting problem which remains to be explained for both systems is the strong predominance of the next-nearest-neighbor (90°) reorientation over the nearest-neighbor (60°) reorientation process. This effect can in no way be understood in terms of a crystal potential of octahedral symmetry for the motion of the Ag^+ ion. An octahedral model potential can be obtained for illustration by developing the crystal potential in spherical harmonics and using the first two terms V_4 and V_6.[24] By superposition of these two terms with variable relative strength, a large variety of potentials can be formed with absolute energy minima in the ⟨110⟩ direction. They are all characterized by relative maxima at ⟨111⟩ and ⟨100⟩ directions, and saddle points of variable position on the ridge connecting the ⟨100⟩ and ⟨111⟩. 60° tunneling through the barrier near this saddle point should, therefore, always be easier than 90° tunneling through the barrier near the ⟨100⟩ maximum. For the extreme case that the saddle point lies near or at the ⟨100⟩ maximum, the path length and barrier height for 60° and 90° tunneling would be comparable. Therefore, as stated first by Silsbee,[20] for all octahedral potentials ⟨110⟩ dipoles should have a larger (or in the limit equal) 60° tunneling matrix element compared to that of 90° tunneling. By the same arguments used above, this statement can be extended to the classical reorientation process. The activiation energy for thermally activated 60° reorientation should always be smaller or equal to that of the 90° reorientation process. While this rule was obeyed by the ⟨110⟩ dipole systems investigated so far (like the O_2^- ions), it is clearly violated by the off-center Ag^+ systems.

By the work of Pirc and Gosar[25] and Shore,[26] it has been clearly shown that the simple picture of a tunneling defect in an octahedral potential, used so far, is inadequate. It neglects completely the

anisotropic elastic distortions, which the defect itself introduces into the cubic lattice surrounding. In the reorientation process, not only the "naked dipole," but the dipole with a "dressing" of lattice distortions has to be reoriented. The effect of this dressing can be regarded as a contribution to the moment of inertia I of the rotating defect, which changes the original value for the naked dipole (I) into a larger "effective" moment of inertia (I^*). For O_2^- molecules, one determines $I^*/I \approx 5$, which shows the predominant importance of the dressing effect in determining reorientation rates.[19] The observed strong variation of the OH^- relaxation time with host materials indicates the same behavior for this system.[22] Within the tunneling model, the dressing effect gives rise to a renormalization factor to the tunneling matrix element, which represents the reorientation of the lattice distortions.[25,26]

The anisotropic lattice distortions around the defect are directly related to the components of the elastic-dipole tensor of the defect. For a [110] defect there are three components of this strain tensor: λ_{110}, the strain parallel to the [110] dipole axis, and $\lambda_{1\bar{1}0}$ and λ_{001}, the strain components in the two directions perpendicular to the dipole axis. The relative sizes of these components will determine the shape factor of the defect, the coupling strength of the defect to strain and phonons of different symmetry, and the size of the dressing effect for different rotations of the defect. Two limiting cases can be differentiated:

a. $|\lambda_{110} - \lambda_{1\bar{1}0}| > |\frac{1}{2}(\lambda_{110} + \lambda_{1\bar{1}0}) - \lambda_{001}|$. For this case the defect couples predominantly to stress and elastic waves of T_{2g} symmetry. The effective moment of inertia will be larger for 90° reorientation than for 60° reorientation.

b. $|\frac{1}{2}(\lambda_{110} + \lambda_{1\bar{1}0}) - \lambda_{001}| > |\lambda_{110} - \lambda_{1\bar{1}0}|$. For this case the defect behaves similarly to the ⟨100⟩ elastic dipole, coupling predominantly to stress of E_g symmetry. 90° reorientation will be affected only by a small dressing factor compared to 60° reorientation.

The second case offers an attractive possibility to explain the predominance of the 90° reorientation by the fact that the defect possesses a considerably larger effective moment of inertia I^* for 60° rotation, compared to 90° rotation [$I^*(60°) > I^*(90°)$]. To phrase it in somewhat different words, a particular [110]-oriented Ag^+ ion introduces a strong tetragonal (E_g) distortion perpendicular to its axis in the [001] direction. This distortion remains constant under 90° dipole reorientation; it, therefore, "traps" the dipole in that particular (001) plane, allowing relatively easy rotation within this plane. 60° reorientation of the dipole requires a change of the plane, i.e., a reorientation of the strong tetragonal distortion. Elasto-optical measurements on the Ag^+ uv absorption are under way to determine accurately the E_g and T_{2g} components of the elastic-dipole tensor, so that this model could be tested and treated quantitatively.

V. COMPARISON OF DERIVED Ag^+ OFF-CENTER MODEL WITH OTHER EXPERIMENTS

For the RbBr: Ag^+ system it is evident now why earlier low-temperature paraelectric experiments gave negative results. Even the rapid 90° reorientation is too slow ($\tau_{pol} \approx 10^2$ sec at 1.3 °K) to show up in normal dielectric or electrocaloric experiments. For the same argument, specific-heat experiments with the usual technique would be expected to miss nearly completely the low-temperature anomaly from the tunneling states.

For the RbCl: Ag^+ system, the situation is more complicated and confusing due to the fact that the time constant of the 90° reorientation is short; that of the 60° reorientation, however, is comparable or long against the time constant of most low-temperature experiments. Many of the contradictions and discrepancies mentioned in Sec. I can be traced to originate from this.

A. Electrocaloric Experiments

The measured electrocaloric effect,[5] reproduced again in Fig. 10, showed a considerably higher saturation value for ⟨111⟩ fields compared to ⟨100⟩ fields, in apparent agreement with a ⟨111⟩ dipole model. These experiments were performed with a switching time of the electric field $\tau_E \approx 10^{-2}$ sec; this was long compared to the electrocalorically determined relaxation time $\tau_R \approx 10^{-5}$ sec, so that the necessary condition for reversible entropy changes $\tau_E > \tau_R$ seemed to have been fulfilled in this experiment. This, however, was true only for the rapid (90°) part of the relaxation. For the slow 60° process, which from our optical data and reorientation kinetics is expected to have a dielectric relaxation time $\tau(60°) \approx 3 \times 10^{-2}$ sec at 1.3 °K, the condition for reversible entropy changes was *not* fulfilled; instead we had $\tau_E < \tau(60°)$.

We, therefore, analyze the old electrocaloric data now in terms of our new model in the following way: For E_{111}, where only the rapid relaxation occurs (Fig. 7), we adjust a calculated curve for ⟨110⟩ dipoles to the measured curve and obtain a good fit with $p = 0.78\ e$ Å (Fig. 10). For the same ⟨110⟩ dipole we give the predicted behavior in ⟨100⟩ and ⟨110⟩ fields (full curves in Fig. 10), calculated for the condition $\tau_e >$ all dipole relaxation times. Our measured curve for E_{100} clearly does not agree with this. If we, however, assume that for the 60° reorientation $\tau_E < \tau(60°)$, so that we missed this part in the cooling experiment, the calculated behavior in ⟨100⟩ and ⟨110⟩ fields becomes changed

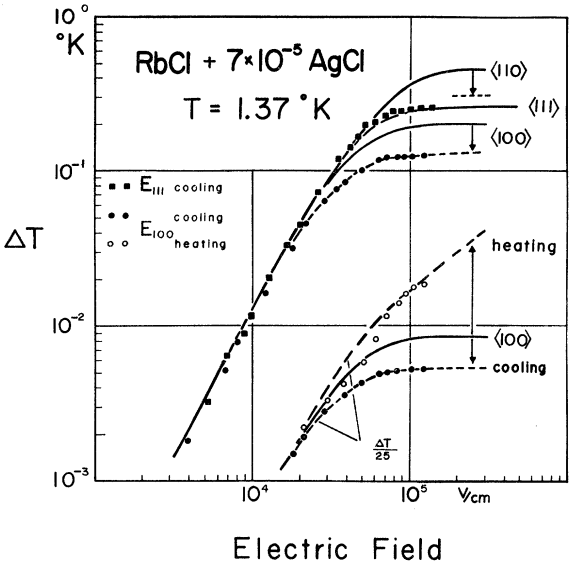

FIG. 10. Electrocaloric effects in RbCl : Ag^+ as a function of E. (a) In the left-hand set of curves, the measured cooling effect under ⟨100⟩ and ⟨111⟩ fields is displayed. The full curves are calculated for ⟨110⟩ dipoles and ⟨100⟩, ⟨110⟩, and ⟨111⟩ fields, with the ⟨111⟩ field curve adjusted to the ⟨111⟩ measurement (adjustment parameter $p = 0.78\ e$ Å). The dotted curves and arrows show how the calculated behavior changes for $\tau_E < \tau(60°)$. (b) The right-hand set of curves (ΔT scale reduced by a factor 25) show the measured heating and cooling effect in ⟨100⟩ fields. The full curve gives the calculated behavior for ⟨110⟩ dipoles, while the dotted curves display the expected changes in heating and cooling for $\tau_E < \tau(60°)$.

into the dotted curves. Now our measured ⟨100⟩ field curve agrees fully with the prediction.

While the cooling effect under ($E_{100} \rightarrow 0$) becomes reduced, the heating effect under ($0 \rightarrow E_{100}$) should become increased as a consequence of $\tau_E < \tau(60°)$, because the levels are completely split by the field before relaxation occurs. Such an asymmetry in the heating and cooling effect was actually observed for E_{100} (right-hand set of curves in Fig 10), and can be well fitted with the calculated behavior (dotted curves) obtained for the condition $T_E \ll \tau$ (60°).

B. Dielectric Experiments

It is highly probable that the dielectric measurements[10] (which are normally performed with frequencies not smaller than 100 sec^{-1}) were misled by the same time-constant effect. If the slow 60° reorientation process is missed (for ⟨100⟩ or ⟨110⟩ fields), the total polarization will appear to be largest in ⟨111⟩ fields, leading to the erroneous conclusion that the dipoles lie in ⟨111⟩ directions.

C. Specific-Heat Experiments

It is not known how the temperature dependence of 60° reorientation time in RbCl: Ag^+ proceeds beyond 1.8 °K. Assuming, however, a linear extrapolation of the curve in Fig. 8, one would obtain $\tau \approx 10^4$ sec at 0.1 °K. This would mean that the specific-heat experiment of Rollefson[11] (performed with a time constant of about 10 sec) would have missed a good part of the 60° reorientation processes. The observed shape of the anomaly would be strongly affected by cutting it off to low temperatures, and the integrated entropy change ΔS would be reduced. This may partly explain the small ΔS value obtained in Ref. 11.

D. Paraelectric Resonance

The conclusion from the PER work[7] left two alternatives: (i) ⟨111⟩ dipoles with nearest-neighbor tunneling; and (ii) ⟨110⟩ dipoles with next-nearest-neighbor tunneling. Our model clearly decides for the second alternative.

E. Elastic-Dipole Properties

The briefly reported result from elastic measurements,[10] that the elastic-dipole moment of Ag^+ in RbCl has mainly ⟨100⟩ symmetry, is not contradictory to our ⟨110⟩ electric-dipole model, but is in fact an expected feature, which is needed to explain the particular reorientation properties of the defect, as discussed in Sec. IV.

ACKNOWLEDGMENTS

The authors are indebted to Dr. Conrad Miziumski for clarifying suggestions concerning the relaxation kinetics, and to Dr. Rasa Pirc for several valuable and critical discussion on this work.

---

†Work supported in part by the AFOSR, under Grant No. 69-1649.

*Present address: Dept. de Fisica, Escola de Engenharia, São Carlos, Est. São Paulo, Brazil.

[1]For a recent review of the off-center properties of Li^+ in KCl, see V. Narayanamurty and R. O. Pohl, Rev. Mod. Phys. 42, 201 (1970).

[2]K. Fussgaenger, Phys. Status Solidi 34, 157 (1969); 36, 645 (1969).

[3]E. Krätzig, T. Timusk, and W. Martienssen, Phys. Status Solidi 10, 709 (1965).

[4]W. Dreybrodt and K. Fussgaenger, Phys. Status Solidi 18, 133 (1966).

[5]S. Kapphan and F. Lüty, Solid State Commun. 6, 907 (1968).

[6]W. D. Wilson, R. D. Hatcher, R. Smoluchowski, and G. J. Dienes, Phys. Rev. 184, 844 (1969).

[7]F. Bridges, Phys. Status Solidi (to be published).

[8]I. G. Nolt, Ph.D. thesis (Cornell University, 1967) (unpublished).

[9]R. D. Kirby, A. E. Hughes, and A. J. Sievers, Phys. Rev. B 2, 481 (1970).

[10]R. C. Hanson, H. Shuman, and J. R. Hallberg, Bull. Am. Phys. Soc. 17, 144 (1972).

[11]R. J. Rollefson, Ph. D. thesis (Cornell University, 1971) (unpublished); and Phys. Rev. (to be published).
[12]R. Sittig, doctoral thesis (University of Frankfurt, 1970) (unpublished).
[13]W. Dultz and Ch. Uihlein (private communication).
[14]U. Kuhn and F. Lüty, Solid State Commun. 2, 281 (1964).
[15]S. Kapphan and F. Lüty, Solid State Commun. 8, 349 (1970).
[16]S. Kapphan, Ph. D. thesis (University of Utah, 1970) (unpublished).
[17]F. Rosenberger, Mater. Res. Bull. 1, 55 (1966).
[18]B. G. Dick, Phys. Status Solidi 29, 587 (1968).
[19]W. Känzig, J. Phys. Chem. Solids 23, 479 (1962); and G. Pfister and W. Känzig, Physik Kondensierten Materie 10, 231 (1969).
[20]R. H. Silsbee, J. Phys. Chem. Solids 28, 2525 (1967).
[21]B. G. Dick and D. Strauch, Phys. Rev. B 2, 2200 (1971).
[22]S. Kapphan, Diplom-thesis (University of Stuttgart, 1966) (unpublished).
[23]H. U. Bosshard, R. W. Dreyfus, and W. Känzig, Physik Kondensierten Materie 4, 254 (1965).
[24]M. T. Hutchings, Solid State Phys. 16, 227 (1964).
[25]P. Gosar and R. Pirc, in *Proceedings of the International Conference on Magnetic Resonance and Relaxation, Fourteenth Colloque Ampère, Ljubljana, Yugoslavia, September*, 1966, edited by R. Blinc (North-Holland, Amsterdam, 1968), p. 636; and R. Pirc and P. Gosar, Physik Kondensierten Materie 9, 377 (1969).
[26]H. B. Shore, Phys. Rev. Letters 17, 1142 (1966).

PHYSICAL REVIEW B VOLUME 6, NUMBER 4 15 AUGUST 1972

Calculation of Reorientation Rates of OH^- Defects in RbBr Using Accurate Phonon Spectra

Herbert B. Shore*
Department of Physics, University of California, San Diego, La Jolla, California 92037
and
Leonard M. Sander
Department of Physics, University of Michigan, Ann Arbor, Michigan 48104
(Received 31 January 1972)

In a recent experiment Kapphan and Lüty measured the reorientation rate of OH^- defects in RbBr in the temperature range 1–15 °K. In this paper we present a theoretical calculation of the reorientation rate in which we treat the defect-lattice coupling and the lattice frequency spectrum as accurately as possible. The coupling is assumed to contain a strain-dipole component and an electric-dipole component; the magnitudes of the two components and the "bare" tunneling matrix element provide three parameters which are adjusted to produce the best agreement with experiment. The lattice spectrum is calculated using shell-model parameters chosen to agree with recent neutron-diffraction data on phonons in RbBr. The relaxation rate is calculated to all orders in the number of phonons. The temperature dependence of the renormalized tunneling matrix element is included. Calculated reorientation rates are in excellent agreement with experiment, but there is no unique choice of the parameters that produces a best fit. The results indicate that at low temperatures the rate is controlled by strain-dipole single-phonon processes and that at high temperatures electric-dipole multiphonon processes are dominant. Plausibility arguments are used to choose a "most probable" set of parameters that is consistent with the reorientation data, and this choice is in satisfactory agreement with values of the parameters obtained from the measured external electric-dipole moment and stress-splitting factor.

I. INTRODUCTION

It has been recognized for several years that a study of reorientation rates of paraelectric[1–4] and paraelastic[5–10] defects in alkali halides could provide information on the nature of the defect-lattice interaction. The role of one-phonon processes in the relaxation of defects such as OH^- in KCl is fairly well understood,[3] but all attempts (including the present one) to include multiphonon processes[11,12] have had to deal with several difficulties. First, the contribution of multiphonon processes is very sensitive to the exact form of the phonon spectrum, so that calculations using a simplified (i.e., Debye) spectrum cannot accurately reproduce experimental results. Similarly, calculated relaxation rates are sensitive to the assumed form of the defect-lattice interaction. Since one wants to use as few adjustable parameters as possible to describe this interaction, a certain amount of guesswork must be used in deciding on a proper form for the interaction. Further, a consistent calculation of multiphonon effects must include the renormalization of the tunneling matrix element[7,8,13–15]; previous calculations that did employ accurate phonon spectra did not take this ef-